JACS
JOURNAL OF THE AMERICAN CHEMICAL SOCIETY

Article

pubs.acs.org/JACS

Atomic-Scale Insight into Tautomeric Recognition, Separation, and Interconversion of Guanine Molecular Networks on Au(111)

Chi Zhang, Lei Xie, Likun Wang, Huihui Kong, Qinggang Tan, and Wei Xu*

Tongji-Aarhus Joint Research Center for Nanostructures and Functional Nanomaterials, College of Materials Science and Engineering, Tongji University, Caoan Road 4800, Shanghai 201804, People's Republic of China

Supporting Information

ABSTRACT: Although tautomerization may directly affect the chemical or biological properties of molecules, real-space investigation on the tautomeric behaviors of organic molecules in a larger area of molecular networks has been scarcely reported. In this paper, we choose guanine (G) molecule as a model system. From the interplay of high-resolution scanning tunneling microscopy (STM) imaging and density functional theory (DFT) calculations, we have successfully achieved the tautomeric recognition, separation, and interconversion of G molecular networks (formed by two tautomeric forms G/9H and G/7H) with the aid of NaCl on the Au(111) surface in ultrahigh vacuum (UHV) conditions. Our results may serve as a prototypical system to provide important insights into tautomerization related issues, which should be intriguing to biochemistry, pharmaceutics, and other related fields.

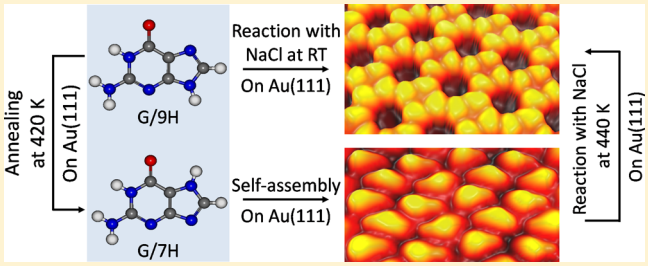

INTRODUCTION

Tautomerization of organic molecules, which involves migration of a hydrogen atom or proton and subsequent interconversion of constitutional isomers, is proven to be of great importance in directly affecting the chemical or biological properties of molecules.[1−5] Such tautomerization phenomenon also extensively exists in DNA bases resulting in the presence of a variety of noncanonical tautomeric forms which may be responsible for base mismatch, mutagenesis, and further genetic damage.[1,2,6,7] Moreover, the rapid interconversion also leads to the coexistence of different tautomers with altered properties, which is an obstacle for the further synthesis and purification. Therefore, tautomerization related issues are fundamentally important and challenging within diverse chemistry subdisciplines from conventional organic chemistry, biochemistry, over pharmaceutical chemistry to the emerging surface chemistry. Relevant spectroscopic and theoretical studies on the possible tautomeric forms and their stabilities were performed, and tautomeric identification and separation were also achieved in the past few years.[8−14] Recently, on-surface tautomerization processes have also been explored in ultrahigh vacuum (UHV) conditions and mainly concentrated on the systems of (1) free-based naphthalocyanine,[15] phthalocyanine,[16] porphyrin,[17] and diamine[18] molecules triggered by electron injection; (2) porphycene molecule[19,20] induced by the single atoms or molecules located nearby or induced via the excitation of specific molecular vibrations or thermal activation. The previous studies mentioned above were mainly focused on the tautomerization of single molecules. However, simultaneous tautomerization of a whole molecular network, to our knowledge, has been scarcely reported to date. It is therefore of great interest and also challenging to systematically explore in real space the tautomeric recognition, separation and interconversion in a larger area of molecular networks in a facile manner, which is complicated for the traditional experimental methods yet crucial to biochemistry, pharmaceutics and other related fields.

Guanine (G) molecule is known to have many different tautomers and the two most stable ones are the canonical G/9H form and the noncanonical G/7H form[8,9,21] as shown in Scheme 1. It thus may provide us a model system to investigate the tautomerization related fundamental issues of G molecules on a solid surface. Based on the previous literatures[22−27] and also specifically our own work,[28] it is known that (1) NaCl islands grown on substrates can be employed as a sort of reactant to effectively interact with the guanine derivative resulting in the formation of G-quartet-Na complex; (2) G-quartet structure can only be formed by the canonical form (G/9H). Thus, in this study, we try to explore the feasibility of using NaCl as an aid (by facilitating the formation of G-quartet-Na structure) to achieve tautomeric recognition, separation and interconversion of G molecular networks (formed by two tautomeric forms G/9H and G/7H) on a Au(111) surface. For this kind of study, scanning tunneling microscopy (STM) has proven to be the technique of choice, since it allows a direct, real-space determination of surface molecular nanostructures with submolecular resolution.[24−35] From the interplay of high-resolution STM imaging and density functional theory (DFT) calculations, we have successfully achieved the following. (1)

Received: July 14, 2015
Published: August 31, 2015

DOI: 10.1021/jacs.5b07314
J. Am. Chem. Soc. 2015, 137, 11795−11800

Scheme 1. Schematic Illustration on the Formation of G-Quartet-Na Network Structure (Composed of the Canonical G/9H Form) and the Formation of a Close-Packed Noncanonical G/7H Structure on Au(111), and the Interconversion between G/9H and G/7H

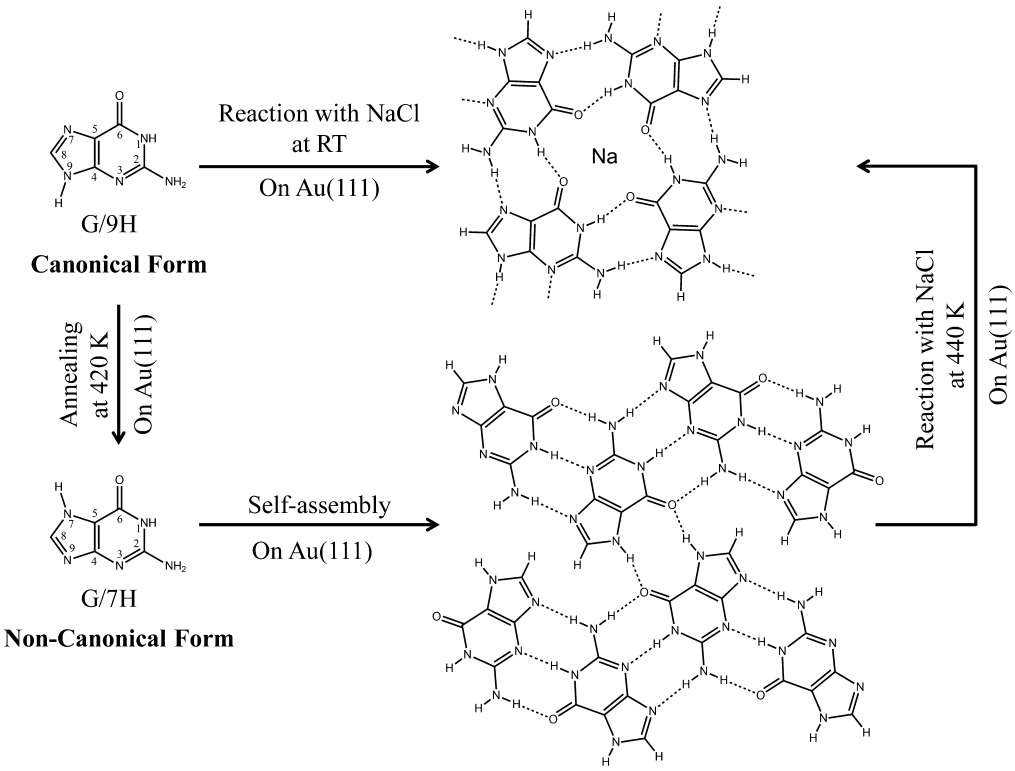

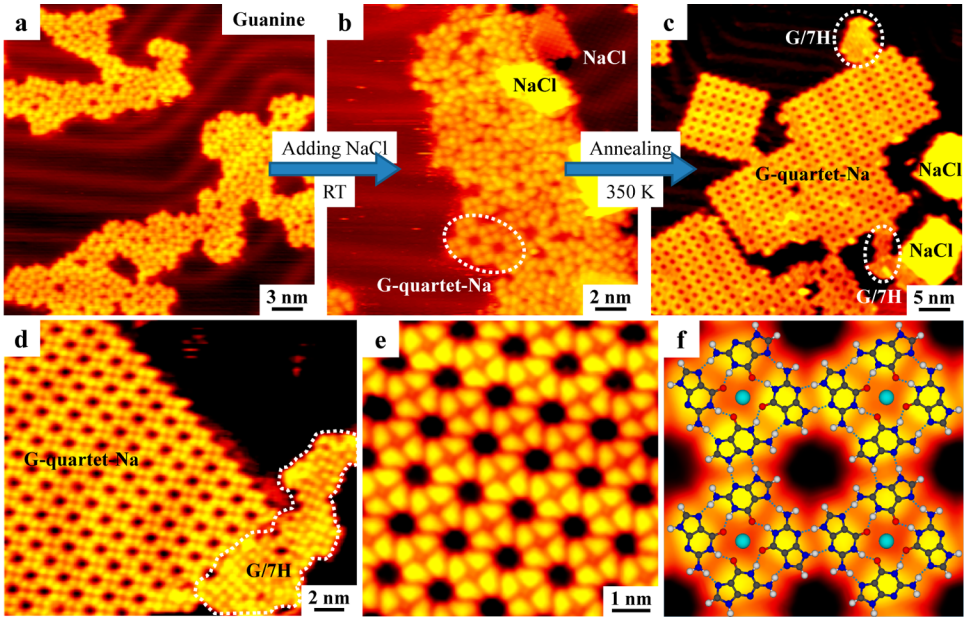

Figure 1. STM images and DFT-optimized structural model showing the formation of predominant G-quartet-Na network structure coexisting with small patches of close-packed G/7H structure on Au(111) with the aid of sufficient NaCl (the NaCl/guanine ratio is higher than 1:4). (a) STM image showing the formation of disordered nanostructures after deposition of G molecules on Au(111) at RT. (b) STM image showing the appearance of a small island of G-quartet-Na structure after deposition of NaCl on the G-molecule-covered surface at RT. (c) Large-scale STM image showing the formation of predominant G-quartet-Na network together with small patches of close-packed G/7H structure after gentle annealing of the sample at 350 K. (d) Zoom-in STM image showing the coexistence of the G-quartet-Na network and the close-packed G/7H island. (e, f) Close-up high-resolution STM images of the G-quartet-Na network with the DFT-optimized structural model superimposed, where hydrogen bonds are depicted by dashed lines. H, white; C, gray; N, blue; O, red; Na, azure. Scanning conditions: I_t = 0.6 nA, V_t = −1.2 V.

Recognition and separation of the two G tautomers from a mixture phase: the G/9H molecules form the G-quartet-Na structure[28] with the aid of NaCl, while the G/7H ones form the close-packed structure.[21] (2) Interconversion between G/9H

DOI: 10.1021/jacs.5b07314
J. Am. Chem. Soc. 2015, 137, 11795−11800

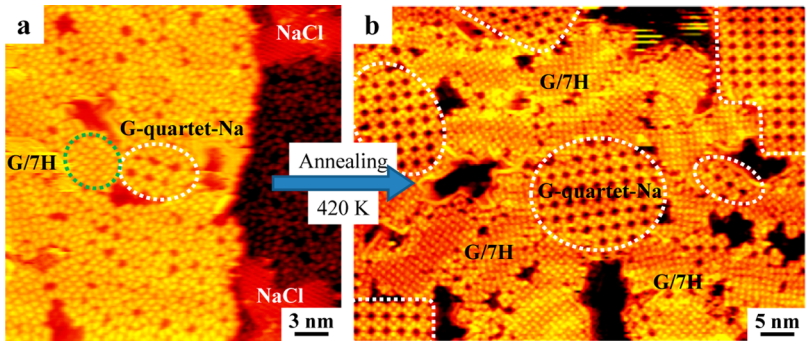

Figure 2. STM images showing the formation of comparatively large islands of close-packed G/7H nanostructure with small islands of G-quartet-Na network structure on Au(111) when NaCl is insufficient (the NaCl/guanine ratio is much lower than 1:4). (a) STM image showing the coexistence of small islands of G-quartet-Na and G/7H structures (highlighted by the white and green ovals, respectively) with the remaining disordered phases after deposition of small amounts of NaCl on Au(111) at RT and further annealing at 350 K. (b) STM image showing the coexistence of comparatively large islands of G/7H structure and patches of G-quartet-Na structure (highlighted by the white contours) after subsequent annealing the sample at 420 K. Scanning conditions: I_t = 0.8 nA, V_t = −1.2 V.

and G/7H forms: G/9H can be converted to G/7H by thermal treatment forming a tautomerically pure G/7H phase, and G/7H can be converted back to G/9H which is trapped by NaCl forming a tautomerically pure G-quartet-Na structure. (3) Structural transformation from the G-quartet-Na structure to a more open porous G_3Na_3 one by further reaction with NaCl. These interesting results demonstrate the feasibility of making use of NaCl as an aid to recognize, separate, and even convert different G tautomers in a larger area of molecular networks, which provides important atomic-scale insights into the tautomerization related issues in a variety of fields ranging from organic to surface chemistry.

RESULTS AND DISCUSSION

Note that though it was previously shown that the formation of empty G-quartet network is possible on Au(111),[36,37] it has been indeed very difficult. Instead, we normally get a disordered phase as shown in Figure 1a after deposition of G molecules on Au(111) at room temperature (RT). As mentioned above, we speculate that the difficulty in producing the empty G-quartet structure might be attributed to the influence of tautomerization since it is known that the tautomerization of G molecule extensively exists in the gas phase, aqueous solution and solid state.[8,9] It can also be observed from the STM image that the herringbone reconstruction of the Au(111) surface is not influenced upon the adsorption of G molecules, and the interaction between the G molecule and the surface is mainly vdW forces as reported previously.[37]

After subsequent deposition of sufficient NaCl (the NaCl/guanine ratio is higher than 1:4) at RT, interestingly, a small island of G-quartet-Na structure (highlighted by the white oval) appears as shown in Figure 1b, which is similar to the empty G-quartet[36,37] and the G-quartet-K[38] structures. Furthermore, after gentle annealing of the sample at ∼350 K, surprisingly, we observe the formation of predominant G-quartet-Na structure together with small patches of the close-packed structure as shown in Figure 1c. From a zoom-in STM image (Figure 1d) we could identify the details of the close-packed structure and assign it to the G/7H phase (highlighted by the white contour). The typical zoom-in STM image of the small patch (as shown in Figure S1) is completely consistent with the DFT-optimized G/7H structural model superimposed and also agrees with the STM morphology of the pure G/7H structure as reported previously[21] (also shown in Figure S2). Close-up high-resolution STM images of the G-quartet-Na network structure (where Na is visible as a dot in the center which is more clearly resolved in Figure S3) with the DFT-optimized model superimposed are shown in Figure 1e, f. Comparison of the relaxed gas-phase model with the experimental STM image shows a good agreement. Similar to the mechanism proposed in our previous work,[28] we identify that the formation of the G-quartet-Na networks is attributed to the cooperative effect of intraquartet hydrogen bonding and electrostatic ionic bonding, and additionally, the interquartet hydrogen bonding further stabilizes the whole network structure, resulting in a quite high binding energy of 1.90 eV/molecule from our DFT calculations. Note that in this process the annealing temperature (∼350 K) is much lower than that for inducing on-surface tautomerization from G/9H to G/7H (which takes place at ∼420 K),[21] therefore the G/7H phase observed during this process originates from the initially existing G/7H molecules in the disordered phase. Thus, with the aid of NaCl, we have successfully achieved recognition and separation of the two G tautomers (i.e., G/9H and G/7H) from a disordered phase by forming a G-quartet-Na structure and a close-packed G/7H structure, respectively.

To further verify the necessity of NaCl in the process of tautomeric recognition and separation, a control experiment with insufficient NaCl dosage (the NaCl/guanine ratio is much lower than 1:4) has been performed. After deposition of small amounts of NaCl followed by G molecules on the surface at RT and subsequent annealing at 350 K, coexistence of small islands of G-quartet-Na and G/7H structures with the remaining disordered phase is observed as shown in Figure 2a. Due to the relatively high total surface coverage of both G molecules and NaCl (∼0.9 ML), diffusion of G molecules and NaCl may be limited resulting in the incomplete reaction. After further annealing the sample at 420 K (the temperature for G tautomerization from G/9H to G/7H), as expected, all of the NaCl islands are consumed by interacting with G/9H molecules forming G-quartet-Na islands, and moreover, the remaining unreacted G/9H molecules are converted to G/7H ones together with the original G/7H molecules forming the comparatively large islands as shown in Figure 2b. It is worthwhile to note that no structural transformation is observed after further annealing such a sample up to the temperature of 500 K (as shown in Figure S4) (then both structures desorb from the surface). Moreover, STM images

DOI: 10.1021/jacs.5b07314
J. Am. Chem. Soc. 2015, 137, 11795−11800

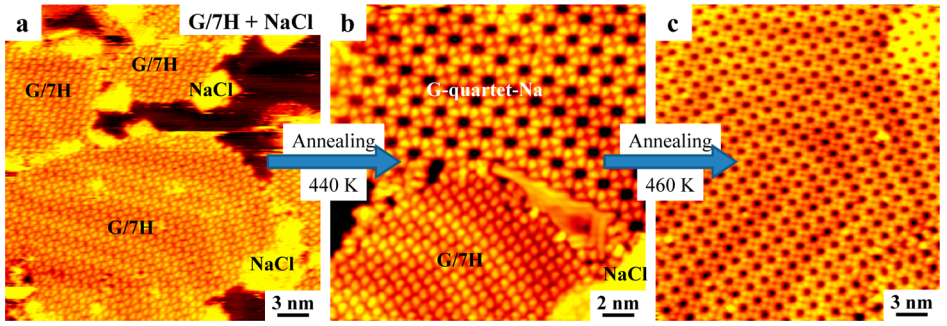

Figure 3. STM images showing the complete conversion from close-packed G/7H nanostructure to G-quartet-Na network structure on Au(111) when the NaCl/guanine ratio is higher than 1:4. (a) STM image showing the coexistence of close-packed G/7H nanostructure merely and NaCl islands at RT. (b) STM image showing the formation of G-quartet-Na network structure with the remaining G/7H nanostructure after subsequent annealing the sample at 440 K. (c) STM image showing the formation of entire G-quartet-Na network structure after further annealing the sample at 460 K. Scanning conditions: I_t = 0.6 nA, V_t = −1.2 V.

obtained after deposition of NaCl and G molecules with different ratios and further thermal treatment at 420 K have also been shown in Figure S5. Based on the above, we could draw the conclusion that when NaCl is sufficient, all of the G/9H molecules can be recognized and separated from G/7H ones in a mixture phase, however, when NaCl is insufficient, only part of the G/9H molecules can be separated and the remaining ones are forced to convert to G/7H form after thermal treatment.

As it is known that G/9H can be converted to G/7H,[21] a step further, it is of utmost interest to explore the feasibility of reversing the conversion. We then first deposit G molecules on the surface followed by subsequent annealing at ∼420 K which results in the formation of the tautomerically pure G/7H structure as reported previously[21] (also shown in Figure S2). After further introduction of sufficient NaCl (the NaCl/guanine ratio is higher than 1:4) onto the G/7H-covered sample at RT (Figure 3a) followed by annealing at 440 K, surprisingly enough, we observe the formation of G-quartet-Na network structure coexisting with the remaining G/7H structure as shown in Figure 3b. Higher annealing temperature of 460 K results in a complete conversion from the G/7H structure to the G-quartet-Na structure (Figure 3c). Thus, we assume that at high temperatures two tautomeric forms G/9H and G/7H keep on interconverting with migration of a hydrogen atom or proton. Once the G/9H form encounters NaCl, it will be trapped by forming the thermodynamically more stable G-quartet-Na structure. If there is no NaCl, during cooling down of the sample G/7H form is trapped via the formation of the close-packed structure (with binding energy of 1.4 eV/molecule as reported, which is more stable than the empty G-quartet network without metal center by ∼0.3 eV/molecule).[21] In view of the above, we conclude that the tautomeric conversion from G/7H to G/9H is also feasible with the aid of NaCl where formation of the G-quartet-Na structure is the key to allowing the G/9H form to be trapped in this process. Thus, the tautomerization process between G/9H and G/7H is proven to be reversible.

As the G/9H form is sensitive to NaCl, to gain further insight into the interaction between G molecules and NaCl, we have also managed to prepare a tautomerically pure G-quartet-Na structure followed by dosing sufficient NaCl (the NaCl/guanine ratio is higher than 1:1) as shown in Figure 4a. Interestingly, further thermal treatment at ∼520 K results in the structural transformation from the G-quartet-Na structure to a more open porous structure as shown in Figure 4b. A close-up

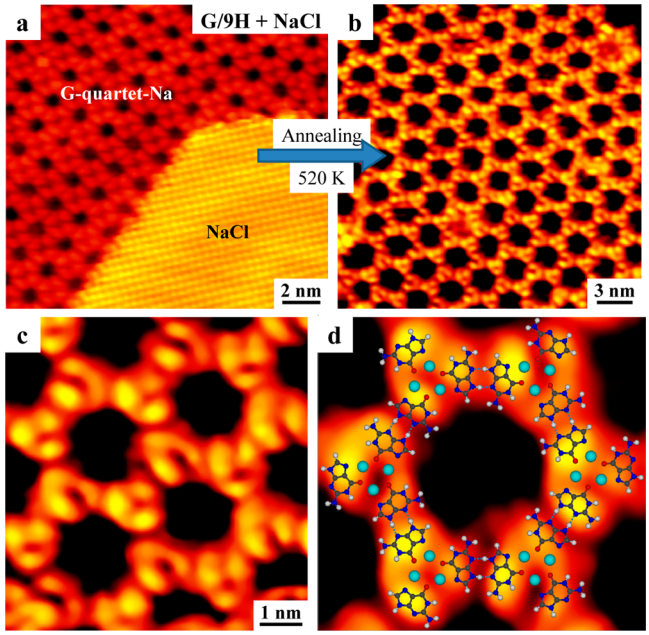

Figure 4. STM images showing the transformation from the G-quartet-Na structure to a more open porous structure on Au(111) when further reacting with NaCl. (a) STM image showing the coexistence of the G-quartet-Na structure and the NaCl island at RT. (b) Large-scale STM image showing the formation of a new porous structure after annealing the sample at 520 K. (c, d) Close-up high-resolution STM images of the porous structure with the DFT-optimized gas-phase model superimposed, where hydrogen bonds are depicted by dashed lines. H, white; C, gray; N, blue; O, red; Na, azure. Scanning conditions: I_t = 1.0 nA, V_t = −1.2 V.

high-resolution STM image shown in Figure 4c provides more details where the triangular elementary structural motif can be identified, which is similar to the G_3K_2 motif reported previously.[39] To gain atomic-scale insight into this new structure, further DFT calculations are performed. As shown in Figure 4d, a relaxed gas-phase model is superimposed on a close-up STM image where a good agreement is achieved. From the model we identify that the elementary motif is composed of three G/9H molecules and three Na binding together via electrostatic ionic bonding between Na and O/N, and intermolecular hydrogen bonds further link the triangular motifs into this porous structure. Such metal−organic motif is similar to the reported structures based on three-metal

DOI: 10.1021/jacs.5b07314
J. Am. Chem. Soc. 2015, 137, 11795−11800

center[40−42] and the formed structure is the balance between the electrostatic ionic bonding and the Na−Na electrostatic repulsion. From the DFT calculations, we obtain the binding energy of this structure (∼1.96 eV/molecule), which is slightly more stable than the G-quartet-Na structure (∼1.90 eV/molecule) indicating that this structural transformation is a thermodynamic process, and this porous structure can endure higher temperatures up to 600 K.

Note that, as reported previously,[24−27] after heating the surface (at ∼400 K or even above), a large amount of Cl species disappeared from the surface and the remaining ones may diffuse into the bulk lattice. Since most of Cl species disappears from the surface, the experimental results in the whole process should be independent of the halide ion used. Also as reported in our recent work,[28] other alkali and alkaline earth salts like KBr and $CaCl_2$ should also be feasible but less efficient for this tautomeric recognition, separation and interconversion scenario. Besides, the charge imbalance in the G-quartet-Na and G_3Na_3 structures may be accommodated in surface studies by charge screening and the presence of image charges in the conductive surface as reported.[25,26]

CONCLUSIONS

In conclusion, from the interplay of high-resolution STM imaging and DFT calculations, we have successfully achieved (1) the tautomeric recognition, separation and interconversion of G molecular networks with the aid of NaCl on the Au(111) surface; (2) the fabrication of tautomerically pure phases, that is, the G-quartet-Na phase and the G/7H close-packed phase, respectively; (3) the structural transformation from a G-quartet-Na structure to a more open porous G_3Na_3 structure by regulating the reaction temperature. These findings may serve as a model system to provide fundamental understandings on both chemically and biologically intriguing topics about tautomerism.

METHODS

All STM experiments were performed in a UHV chamber (base pressure 1×10^{-10} mbar) equipped with a variable-temperature, fast-scanning "Aarhus-type" STM using electrochemically etched W tips purchased from SPECS,[43,44] a molecular evaporator and an e-beam evaporator, and other standard instrumentation for sample preparation. The Au(111) substrate was prepared by several cycles of 1.5 keV Ar^+ sputtering followed by annealing to 800 K for 15 min, resulting in clean and flat terraces separated by monatomic steps. The guanine molecules (purchased from Alfa-Aesar, purity >98%) and NaCl (purchased from Sigma-Aldrich, purity >99%) were loaded into glass crucibles in the molecular evaporator. After a thorough degassing, the G molecules and NaCl were deposited onto the Au(111) substrate by thermal sublimation at 390 and 630 K, respectively, and the sample was thereafter transferred within the UHV chamber to the scanning tunneling microscope, where measurements were carried out at ∼150 K. All the STM images were further smoothed to eliminate noises.

The calculations were performed in the framework of DFT by using the Vienna ab initio simulation package (VASP).[45,46] The projector-augmented wave method was used to describe the interaction between ions and electrons;[47,48] the Perdew−Burke−Ernzerhof GGA exchange-correlation functional was employed,[49] and van der Waals interactions were included using the dispersion-corrected DFT-D2 method of Grimme.[50] The atomic structures were relaxed using the conjugate gradient algorithm scheme as implemented in the VASP code until the forces on all unconstrained atoms were ≤0.03 eV/Å.

ASSOCIATED CONTENT

Supporting Information

The Supporting Information is available free of charge on the ACS Publications website at DOI: 10.1021/jacs.5b07314.

Typical zoom-in STM image of the small patch of close-packed structure after gentle annealing of the sample at 350 K with DFT-optimized G/7H structural model superimposed in a good agreement; STM images showing the formation of close-packed G/7H phase after deposition of G molecules on Au(111) and further annealing at 420 K; close-up STM image showing the G-quartet-Na network where the Na is clearly visible as a dot in the center; STM image showing the thermal stability of the G-quartet-Na network structure and the close-packed G/7H structure after annealing up to 500 K; STM images after deposition of NaCl and guanine molecules with different ratios and further thermal treatment at 420 K (PDF)

AUTHOR INFORMATION

Corresponding Author

*xuwei@tongji.edu.cn

Notes

The authors declare no competing financial interest.

ACKNOWLEDGMENTS

The authors acknowledge financial support from the National Natural Science Foundation of China (21103128, 21473123), the Research Fund for the Doctoral Program of Higher Education of China (20120072110045). Prof. Flemming Besenbacher is acknowledged for fruitful discussion.

REFERENCES

(1) Katritzky, A. R.; Karelson, M. *J. Am. Chem. Soc.* **1991**, *113*, 1561−1566.
(2) Morgan, A. R. *Trends Biochem. Sci.* **1993**, *18*, 160−163.
(3) Llor, J.; Munoz, L. *J. Org. Chem.* **2000**, *65*, 2716−2722.
(4) Bazsó, G.; Tarczay, G.; Fogarasi, G.; Szalay, P. G. *Phys. Chem. Chem. Phys.* **2011**, *13*, 6799−6807.
(5) Peng, C. S.; Tokmakoff, A. *J. Phys. Chem. Lett.* **2012**, *3*, 3302−3306.
(6) Goodman, M. F. *Nature* **1995**, *378*, 237−8.
(7) Wang, W.; Hellinga, H. W.; Beese, L. S. *Proc. Natl. Acad. Sci. U. S. A.* **2011**, *108*, 17644−17648.
(8) Langer, H.; Doltsinis, N. L. *J. Chem. Phys.* **2003**, *118*, 5400−5407.
(9) Lopes, R. P.; Marques, M. P. M.; Valero, R.; Tomkinson, J.; de Carvalho, L. A. *Spectroscopy* **2012**, *27*, 273−292.
(10) Hanus, M.; Ryjácek, F.; Kabelác, M.; Kubar, T.; Bogdan, T. V.; Trygubenko, S. A.; Hobza, P. *J. Am. Chem. Soc.* **2003**, *125*, 7678−7688.
(11) Bazsó, G.; Tarczay, G.; Fogarasi, G.; Szalay, P. G. *Phys. Chem. Chem. Phys.* **2011**, *13*, 6799−6807.
(12) Peng, C. S.; Tokmakoff, A. *J. Phys. Chem. Lett.* **2012**, *3*, 3302−3306.
(13) Allegretti, P. E.; Schiavoni, M. M.; Di Loreto, H. E.; Furlong, J. J. P.; Della Védova, C. O. *J. Mol. Struct.* **2001**, *560*, 327−335.
(14) Shinde, Y.; Sproules, S.; Kathawate, L.; Pal, S.; Konkimalla, V. B.; Salunke-Gawali, S. *J. Chem. Sci.* **2014**, *126*, 213−225.
(15) Liljeroth, P.; Repp, J.; Meyer, G. *Science* **2007**, *317*, 1203−1206.
(16) Sperl, A.; Kröger, J.; Berndt, R. *Angew. Chem., Int. Ed.* **2011**, *50*, 5294−5297.
(17) Auwärter, W.; Seufert, K.; Bischoff, F.; Ecija, D.; Vijayaraghavan, S.; Joshi, S.; Klappenberger, F.; Samudrala, N.; Barth, J. V. *Nat. Nanotechnol.* **2012**, *7*, 41−46.

DOI: 10.1021/jacs.5b07314
J. Am. Chem. Soc. 2015, 137, 11795−11800

(18) Simpson, G. J.; Hogan, S. W.; Caffio, M.; Adams, C. J.; Früchtl, H.; van Mourik, T.; Schaub, R. *Nano Lett.* **2014**, *14*, 634−639.
(19) Kumagai, T.; Hanke, F.; Gawinkowski, S.; Sharp, J.; Kotsis, K.; Waluk, J.; Persson, M.; Grill, L. *Nat. Chem.* **2014**, *6*, 41−46.
(20) Kumagai, T.; Hanke, F.; Gawinkowski, S.; Sharp, J.; Kotsis, K.; Waluk, J.; Persson, M.; Grill, L. *Phys. Rev. Lett.* **2013**, *111*, 246101.
(21) Kong, H.; Sun, Q.; Wang, L.; Tan, Q.; Zhang, C.; Sheng, K.; Xu, W. *ACS Nano* **2014**, *8*, 1804−1808.
(22) Ciesielski, A.; Lena, S.; Masiero, S.; Spada, G. P.; Samori, P. *Angew. Chem., Int. Ed.* **2010**, *49*, 1963−1966.
(23) González-Rodríguez, D.; Janssen, P. G.; Martín-Rapún, R.; Cat, I. D.; Feyter, S. D.; Schenning, A. P.; Meijer, E. W. *J. Am. Chem. Soc.* **2010**, *132*, 4710−4719.
(24) Wäckerlin, C.; Iacovita, C.; Chylarecka, D.; Fesser, P.; Jung, T. A.; Ballav, N. *Chem. Commun.* **2011**, *47*, 9146−9148.
(25) Skomski, D.; Abb, S.; Tait, S. L. *J. Am. Chem. Soc.* **2012**, *134*, 14165−14171.
(26) Skomski, D.; Tait, S. L. *J. Phys. Chem. C* **2013**, *117*, 2959−2965.
(27) Shimizu, T. K.; Jung, J.; Imada, H.; Kim, Y. *Angew. Chem., Int. Ed.* **2014**, *53*, 13729−13733.
(28) Zhang, C.; Wang, L.; Xie, L.; Kong, H.; Tan, Q.; Cai, L.; Sun, Q.; Xu, W. *ChemPhysChem* **2015**, *16*, 2099−2105.
(29) Repp, J.; Meyer, G.; Paavilainen, S.; Olsson, F. E.; Persson, M. *Science* **2006**, *312*, 1196−1199.
(30) Papageorgiou, A. C.; Fischer, S.; Oh, S. C.; Saglam, O.; Reichert, J.; Wiengarten, A.; Seufert, K.; Vijayaraghavan, S.; Ecija, D.; Auwärter, W.; Allegretti, F.; Acres, R. G.; Prince, K. C.; Diller, K.; Klappenberger, F.; Barth, J. V. *ACS Nano* **2013**, *7*, 4520−4526.
(31) Shi, Z.; Liu, J.; Lin, T.; Xia, F.; Liu, P. N.; Lin, N. *J. Am. Chem. Soc.* **2011**, *133*, 6150−6153.
(32) Lin, N.; Dmitriev, A.; Weckesser, J.; Barth, J. V.; Kern, K. *Angew. Chem., Int. Ed.* **2002**, *41*, 4779−4783.
(33) Spillmann, H.; Dmitriev, A.; Lin, N.; Messina, P.; Barth, J. V.; Kern, K. *J. Am. Chem. Soc.* **2003**, *125*, 10725−10728.
(34) Wang, L.; Kong, H.; Zhang, C.; Sun, Q.; Cai, L.; Tan, Q.; Besenbacher, F.; Xu, W. *ACS Nano* **2014**, *8*, 11799−11805.
(35) Zhang, H. M.; Franke, J. H.; Zhong, D. Y.; Li, Y.; Timmer, A.; Arado, O. D.; Monig, H.; Wang, H.; Chi, L. F.; Wang, Z. H.; Müllen, K.; Fuchs, H. *Small* **2014**, *10*, 1361−1368.
(36) Otero, R.; Schöck, M.; Molina, L. M.; Lægsgaard, E.; Stensgaard, I.; Hammer, B.; Besenbacher, F. *Angew. Chem., Int. Ed.* **2005**, *44*, 2270−2275.
(37) Xu, W.; Kelly, R. E.; Gersen, H.; Lægsgaard, E.; Stensgaard, I.; Kantorovich, L. N.; Besenbacher, F. *Small* **2009**, *5*, 1952−1956.
(38) Xu, W.; Tan, Q.; Yu, M.; Sun, Q.; Kong, H.; Lægsgaard, E.; Stensgaard, I.; Kjems, J.; Wang, J.; Wang, C.; Besenbacher, F. *Chem. Commun.* **2013**, *49*, 7210−7212.
(39) Xu, W.; Wang, J. G.; Yu, M.; Lægsgaard, E.; Stensgaard, I.; Linderoth, T. R.; Hammer, B.; Wang, C.; Besenbacher, F. *J. Am. Chem. Soc.* **2010**, *132*, 15927−15929.
(40) Bebensee, F.; Svane, K.; Bombis, C.; Masini, F.; Klyatskaya, S.; Besenbacher, F.; Ruben, M.; Hammer, B.; Linderoth, T. R. *Angew. Chem., Int. Ed.* **2014**, *53*, 12955−12959.
(41) Kong, H.; Wang, L.; Sun, Q.; Zhang, C.; Tan, Q.; Xu, W. *Angew. Chem., Int. Ed.* **2015**, *54*, 6526−6530.
(42) Kong, H.; Wang, L.; Tan, Q.; Zhang, C.; Sun, Q.; Xu, W. *Chem. Commun.* **2014**, *50*, 3242−3244.
(43) Besenbacher, F. *Rep. Prog. Phys.* **1996**, *59*, 1737−1802.
(44) Lægsgaard, E.; Österlund, L.; Thostrup, P.; Rasmussen, P. B.; Stensgaard, I.; Besenbacher, F. *Rev. Sci. Instrum.* **2001**, *72*, 3537−3542.
(45) Kresse, G.; Hafner, J. *Phys. Rev. B: Condens. Matter Mater. Phys.* **1993**, *48*, 13115.
(46) Kresse, G.; Furthmüller, J. *Phys. Rev. B: Condens. Matter Mater. Phys.* **1996**, *54*, 11169.
(47) Blöchl, P. E. *Phys. Rev. B: Condens. Matter Mater. Phys.* **1994**, *50*, 17953.
(48) Kresse, G.; Joubert, D. *Phys. Rev. B: Condens. Matter Mater. Phys.* **1999**, *59*, 1758.
(49) Perdew, J. P.; Burke, K.; Ernzerhof, M. *Phys. Rev. Lett.* **1996**, *77*, 3865.
(50) Grimme, S. *J. Comput. Chem.* **2006**, *27*, 1787−1799.

DOI: 10.1021/jacs.5b07314
J. Am. Chem. Soc. 2015, 137, 11795−11800